Expanding the capabilities of arterial spin labeling MRI

Zhang, X.

Chapter III

Time-efficient measurement of multi-phase arterial spin labeling MR signal in white matter

X. Zhang [1], I. Ronen [1], H.E. Kan [1], W.M. Teeuwisse [1], M. J. P. van Osch [1, 2]

1. Department of Radiology, C. J. Gorter Center for high field MRI, Leiden University Medical Center, Leiden, The Netherlands
2. Leiden Institute for Brain and Cognition, Leiden University, Leiden, the Netherlands

Published on NMR in Biomedicine
NMR Biomed., 29: 1519–1525. doi: 10.1002/nbm.3603

Abstract

White matter (WM) perfusion has great potential as a physiological biomarker in many neurological diseases. Although it has been demonstrated previously that arterial spin labeling magnetic resonance imaging (ASL–MRI) enables the detection of perfusion-weighted signal in most voxels in WM, studies of cerebral blood flow (CBF) in WM by ASL-MRI are relatively scarce because of its particular challenges, such as significantly lower perfusion and longer arterial transit times relative to gray matter (GM). Recently, ASL with a spectroscopic readout has been proposed to enhance the sensitivity for the measurement of WM perfusion. However, this approach suffers from long acquisition times, especially when acquiring multi-phase ASL datasets to improve CBF quantification. Furthermore, the potential increase in the signal-to-noise ratio (SNR) by spectroscopic readout compared with echo planar imaging (EPI) readout has not been proven experimentally. In this study, we propose the use of time-encoded pseudo-continuous ASL (te-pCASL) with single-voxel point-resolved spectroscopy (PRESS) readout to quantify WM cerebral perfusion in a more time-efficient manner. Results are compared with te-pCASL with a conventional EPI readout for both WM and GM perfusion measurements. Perfusion measurements by te-pCASL PRESS and conventional EPI showed no significant difference for quantitative WM CBF values (Student's t-test $p = 0.19$) or temporal SNR ($p = 0.33$ and $p = 0.81$ for GM and WM respectively), whereas GM CBF values ($p = 0.016$) were higher using PRESS than EPI readout. WM CBF values were found to be 18.2 ± 7.6 mL/100 g/min (PRESS) and 12.5 ± 5.5 mL/100 g/min (EPI), whereas GM CBF values were found to be 77.1 ± 11.2 mL/100 g/min (PRESS) and 53.6 ± 9.6 mL/100 g/min (EPI).This study demonstrates the feasibility of te-pCASL PRESS for the quantification of WM perfusion changes in a highly time-efficient manner, but it does not result in improved temporal SNR, as does traditional te-pCASL EPI, which remains the preferred option because of its flexibility in use.

Keywords:
CBF, PRESS, SNR, timeǧencoded pCASL, white matter perfusion

Introduction

Information on cerebral perfusion plays an important role in understanding the mechanisms of cerebrovascular disease. Arterial spin labeling magnetic resonance imaging (ASL-MRI) provides a non-invasive approach for the quantification of perfusion in a clinically feasible scan time of approximately 5 min. So far, the majority of cerebral perfusion measurements by ASL have focused on the cerebral blood flow (CBF) in gray matter (GM), which has been recognized as an important clinical indicator for the diagnosis of many neurological diseases (1), whereas studies on white matter (WM) perfusion are relatively scarce. However, WM perfusion has great potential as physiological biomarker in, for instance, large-vessel occlusive disease, in which WM has been shown to be more vulnerable to infarction than GM (2), but also in patients with multiple sclerosis, in whom decreased WM perfusion has been found (3) and as a potential marker in neurodegenerative diseases (4).

Although ASL-MRI has been widely implemented as a non-invasive imaging technique for the measurement of CBF in GM, WM perfusion measurements have proven to be more difficult (5-7). These difficulties result from the much lower perfusion in WM relative to GM, thereby making the signal-to-noise ratio (SNR) of the measurements close to the detection limit. Furthermore, because of the large difference in contrast between GM and WM perfusion, small changes in WM CBF can easily be overlooked. Separate window leveling of the CBF map may alleviate this problem, but this is not performed frequently. Second, WM exhibits relatively long transit times, resulting in more relaxation of the labeled spins before arriving at the tissue level, leading to even lower ASL signal and SNR. Moreover, the unknown arterial transit times (ATTs) make the quantification of CBF in WM more challenging than in GM. Third, partial volume effects could seriously affect the accurate quantification of WM perfusion (7). Because of the much higher CBF in GM relative to WM, even small contaminations from GM can easily and falsely increase the absolute quantitative CBF values in WM.

To alleviate these challenges, it has been proposed to use a single-voxel point-resolved spectroscopy (PRESS) readout in combination with pulsed ASL [flow-sensitive alternating inversion recovery (FAIR) PRESS] to enhance sensitivity (8). This approach, however, suffers from long acquisition times, i.e. over 1 h to acquire a multi-phase dynamic ASL dataset required for accurate quantification. Moreover, the exact increase in SNR on employing the PRESS readout instead of more common readout strategies, such as echo planar imaging (EPI) and

three-dimensional gradient and spin-echo (3D-GRASE) imaging, has not yet been proven experimentally (8). In this study, in order to address the issue of limited available scan time in clinical settings, we propose the use of time-encoded pseudo-continuous ASL (9,10) in combination with single-voxel PRESS (te-pCASL PRESS), to quantify WM perfusion in a more time-efficient manner compared with FAIR PRESS. te-pCASL enables multi-phase data to be acquired simultaneously within a single scan, whilst conserving SNR, alleviating the need to acquire multiple scans sequentially, as proposed previously by Pohmann (8). Measurement of WM perfusion by te-pCASL PRESS is compared with te-pCASL measurements in combination with a conventional EPI readout. Furthermore, measurements by both approaches were also performed in GM in order to characterize the te-pCASL PRESS approach under high-SNR conditions.

METHODS

Overview

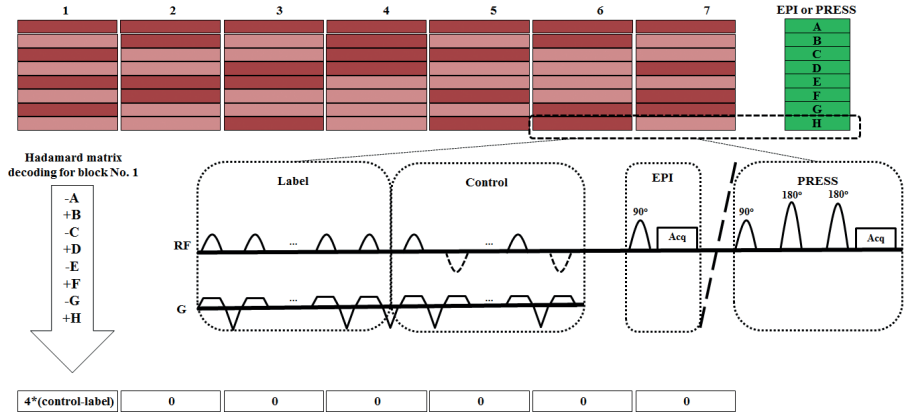

Fig. 1. Sequence diagram of time-encoded pseudo-continuous arterial spin labeling point-resolved spectroscopy (te-pCASL PRESS) and tepCASL echo planar imaging (EPI) with a time-encoded Hadamard matrix of order 8 and a Hadamard decoding scheme for a specific block (block number 1). The red and pink blocks represent the label and control conditions, respectively. When applying this specific decoding scheme, for all blocks except block number 1, the contribution of a specific labeling (control) block is cancelled by the subtraction of the label (control) block of another Hadamard acquisition, resulting in zero net signal. For the first block, a proper ASL signal is obtained (4*control–4*label)

ASL PRESS is based on a conventional ASL preparation in combination with a single-voxel PRESS spectroscopic readout. The ASL signal is subsequently obtained by subtracting the water signal of the label condition from the signal of the control condition, analogous to the normal subtraction of images as performed in standard ASL-MRI. Subsequently, integration of the water signal provides a measure of the local perfusion.

Compared with traditional ASL, the labeling module of te-pCASL is divided into several blocks (also referred to as 'sub-boli'), and the label or control condition of each block is varied according to a Hadamard matrix encoding scheme (Figure 1). Perfusion-weighted images in EPI, or perfusion-weighted spectroscopy signals in PRESS, can be calculated by decoding the Hadamard matrix; by changing the block timings and durations, ASL signals reflecting different post-labeling delays (PLDs) and labeling durations can be obtained. Importantly, the SNRs of ASL signals acquired in this manner are equal to a single PLD experiment with the same labeling duration, PLD and TR, i.e. the information over multiple PLDs can be acquired in the same time and with the same SNR as a single scan with the longest PLD and with the same total number of measurements (e.g. four averages of a traditional pCASL scan have equal SNR to the Hadamard decoded signal of the first block of a Hadamard-8 acquisition).

Subjects

Six healthy volunteers were scanned on a 3-T Achieva MRI scanner (Philips Healthcare, Best, the Netherlands) using a 32-channel receive head coil; one volunteer was scanned with and without vascular crushing to investigate the impact of vascular contamination on the results of the ASL experiments in GM (shown in Supporting Information). Head motion was minimized by means of foam padding. This study was part of a protocol development project approved by the Committee for Medical Ethics of the Leiden University Medical Center, and informed consent was obtained from all subjects.

Acquisition

The encoding scheme of te-pCASL was chosen to be a Hadamard matrix of order 8 using asymmetric and relatively long Hadamard block durations (1500, 1500, 1500, 1500, 1000, 500 and 500 ms) to increase the sensitivity of the detecting of the late-arriving ASL signal in deep WM. The Hadamard scheme containing eight different encodings was repeated 10 times, resulting in a total scan duration of approximately 12.5 min. te-pCASL PRESS, as well as traditional te-pCASL EPI, were performed; for both scans, the interval between the labeling and readout

module was 1000 ms, the excitation flip angle was 90°, linear shimming was performed in the labeling plane and in the region of interest (ROI) separately, and background suppression was included by two spatially selective FOCI pulses at 6600 ms and 7700 ms after the start of labeling (11). For te-pCASL EPI, the following parameters were used: single-shot EPI; EPI factor, 31; sensitivity encoding (SENSE) acceleration factor, 2.5; TE=14 ms; voxel size, 3×3×7 mm^3; five slices, no vascular crushing. For te-pCASL PRESS, the following parameters were used: single-voxel PRESS; first-order pencil-beam shimming (12); spectral bandwidth, 2000 Hz; TE = 36 ms (shortest attainable); number of data points, 1024; no water suppression. A large voxel of (44 ± 4)×(9 ± 0)×(7 ± 0) mm^3 (mean ± standard deviation as calculated over all subjects) was carefully placed within WM in the right hemisphere (Figure 2), and the size of the voxel was adjusted individually as large as possible within the limits of avoiding GM and cerebrospinal fluid contamination, based on a high-resolution three-dimensional T_1 scan (with a spatial resolution of 1.17 × 1.17 × 1.20 mm^3); a similarly sized ROI was selected in GM. Perfusion data as acquired with te-pCASL PRESS were compared with perfusion data from te-pCASL EPI by averaging the imaging data over the same ROIs in post-processing. Equilibrium magnetization (M_0) scans were acquired for both the PRESS and EPI readout.

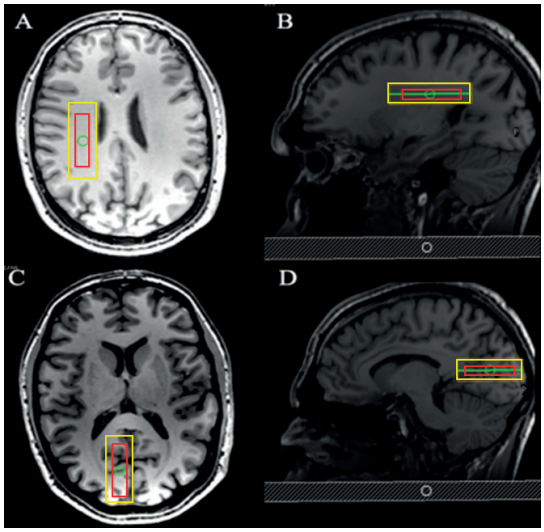

FIG. 2. Planning of region of interest (ROI) in white matter (A, B) and gray matter (C, D) on axial view (A, C) and sagittal view (B, D) of the three-dimensional T_1 image; the red box is the readout volume and the yellow box is the shimming volume

Post-processing

For te-pCASL PRESS, the data were processed using off-line scripts (Matlab, The MathWorks, Natick, MA, USA). The free induction decays (FIDs) of each acquisition of te-pCASL PRESS were phase corrected, filtered with an apodization filter of 20 Hz, four-fold zero filled and Fourier transformed. The resulting water signals were Hadamard decoded and the central 200 points of the Hadamard-decoded water signals were summed for CBF quantification.

Raw images acquired by conventional te-pCASL EPI were first motion corrected. Subsequently, the same Hadamard decoding method as used in the analysis for te-pCASL PRESS was performed using off-line scripts (Matlab, The MathWorks), and signals from the same ROI covering the same anatomical region as in PRESS readout were averaged.

To facilitate easier interpretation, the time courses of the PRESS and EPI perfusion signals were normalized with respect to M_0 and divided by the duration of the specific labeling block. The resulting curves resemble the ASL signal as a function of time obtained by a multi-PLD scan with constant labeling duration (also known as 'Buxton-curves' (13)). The resulting Buxton curves of te-pCASL PRESS were compared with those obtained from te-pCASL EPI. The quantification of CBF was obtained by fitting the time course of perfusion signal to the Buxton model $\Delta M(t) = 2M_0 f\{c(t)*[r(t)m(t)]\}$, where * denotes convolution, $r(t) = e^{-ft/\lambda}$ is the residue function and is the brain-blood partition coefficient, assumed to be 0.90 mL/g in GM and 0.76 mL/g in WM (14); $m(t) = e^{-t/T_1}$ is the magnetization relaxation function with T_1 = 1650 ms; c(t) is the delivery function: $c(t) = \alpha e^{-t/T_1}$ when $\Delta t < t < \tau + \Delta t$ and $c(t) = 0$ when $0 < t < \Delta t$ with $\tau + \Delta t < t$, the labeling efficiency $\alpha = 0.85$, Δt is the ATT and τ is the labeling duration (13). Moreover, the temporal SNR as a function of PLD was calculated for both approaches. The temporal SNR was defined as the (mean signal)/(standard deviation over all repeats).

In order to test whether the quantitative CBF values and temporal SNR derived from the te-pCASL PRESS data were significantly different from those derived from te-pCASL EPI, statistical testing was performed using a Student's paired sample t-test.

RESULTS

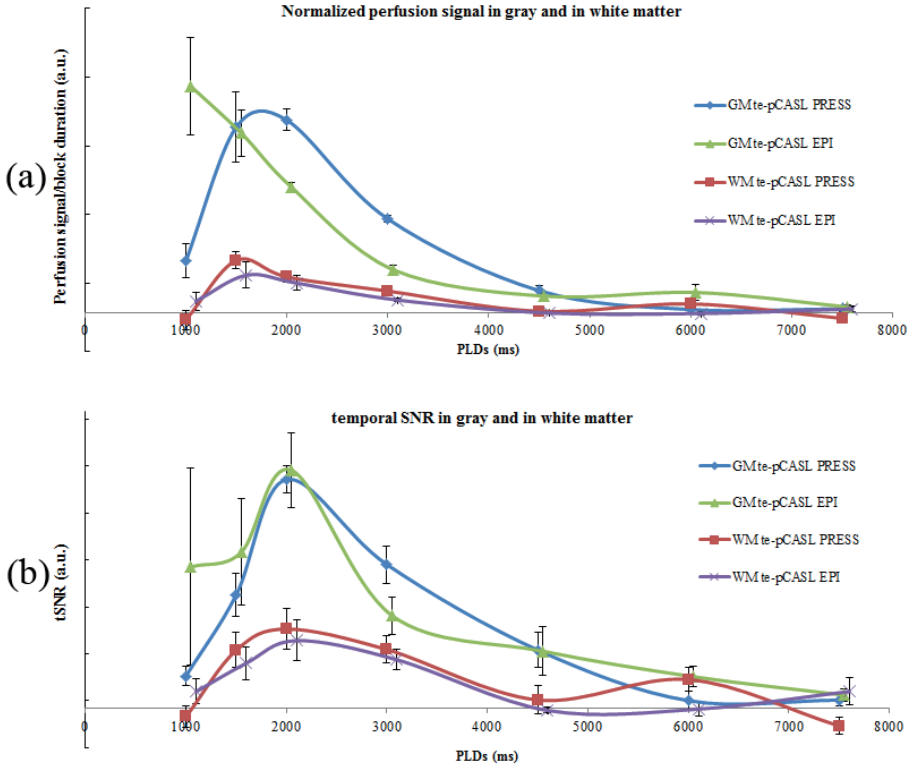

FIG. 3. (a) Time courses of normalized mean perfusion signal and standard error in white (WM) and gray (GM) matter acquired by time-encoded pseudo continuous arterial spin labeling (te-PCASL) point resolved spectroscopy (PRESS) and echo planar imaging (EPI) as calculated over all subjects. The curve acquired by te-pCASL EPI was deliberately shifted to correct for the additional delay in the multi slice readout. (b) Temporal signal to noise ratio (tSNR) as a function of the post labeling delay (PLD) showing similar values for te-pCASL PRESS and te-pCASL EPI

Figure 3a shows the time courses of the normalized perfusion signal (ASL signal divided by M_0 and the duration of the specific labeling block) for te-pCASL PRESS and te-pCASL EPI in WM and GM. For both approaches, the amplitudes of the perfusion signals in WM are much smaller than those in GM, as expected from the lower perfusion. Figure 3b depicts the temporal SNR as a function of PLD showing similar patterns. The temporal SNRs of both approaches were comparable, showing no significant difference with Student's t-test (p = 0.33 and p = 0.81 for GM and WM, respectively).

	CBF (ml/100 g/min)			ATT (ms)			tSNR
	te-pCASL PRESS	**te-pCASL EPI**	**p**	**te-pCASL PRESS**	**te-pCASL EPI**	**p**	**p**
White matter	18.2±7.6	12.5±5.5	0.19	1679 ± 408	1571 ± 297	0.49	0.33
Gray matter	77.1±11.2	53.6±9.6	**0.016**	1579 ± 112	1121 ± 118	**0.000**	0.81

ATT, arterial transit time; CBF, cerebral blood flow; tSNR, temporal signal to noise ratio.

Table 1: Student's paired sample t-test between time-encoded pseudo-continuous arterial spin labeling (te-PCASL) point resolved spectroscopy (PRESS) and te-PCASL echo planar imaging (EPI) (bold type indicates statistically significant at $p < 0.05$)

The quantified CBF values obtained by te-pCASL PRESS were 77.1 ± 11.2 and 18.2 ± 7.6 mL/100 g/min for GM and WM, respectively, whereas the corresponding values for te-pCASL EPI were 53.6 ± 9.6 and 12.5 ± 6.1 mL/100 g/min, respectively (Table 1). The ratios between CBF in GM and WM acquired by te-pCASL PRESS and te-pCASL EPI were 4.24 and 4.29, respectively. The ATTs obtained by te-pCASL PRESS was 1579 ± 112 ms (GM) and 1679 ± 408 ms (WM), whereas they were 1121 ± 118 ms for GM and 1571 ± 297 ms for WM from te-pCASL EPI data (Table 1). No significant differences were found for WM CBF ($p = 0.19$) and WM ATT ($p = 0.49$) acquired by te-pCASL PRESS and te-pCASL EPI. However, GM CBF ($p = 0.016$) and GM ATT ($p = 0.000$) were significantly different between the two approaches (Table 1). All quantified CBF and ATT values are summarized in Table 1.

DISCUSSION

In this study, te-pCASL PRESS was successfully implemented to measure WM perfusion in a time-efficient manner (~12.5 min). WM perfusion measurements by te-pCASL PRESS showed similar temporal SNR relative to conventional EPI. The CBF values in GM were found to be approximately 4.2 times larger than those in WM, both with te-pCASL PRESS and te-pCASL EPI, which is in the expected range and in good agreement with other studies (6,8,15). However, quantitative CBF values and ATTs in GM were higher for the PRESS readout than for the EPI readout.

When comparing the WM results of te-pCASL PRESS with those of te-pCASL EPI, highly similar ASL signal changes as a function of PLD can be observed. In Figure 3a, the two curves are not significantly different from one another for all PLDs, when the 'mean ± 2×standard error' criterion is used as confidence interval. Peak signal is observed at PLD of 1500 ms, after which a rather gradual decrease in normalized ASL signal can be observed. For PLDs of 4500 ms and longer, the ASL signal can no longer be discriminated from zero. In future experiments, it would therefore be more efficient to change the total duration of the Hadamard encoding to a PLD range between 1000 and 4500 ms. This would also significantly shorten the duration of a single acquisition, thereby enabling more averaging in the same total scan time. However, as shorter block durations will also result in lower signal for the decoded ASL signal of that block, comparable temporal SNR is expected for the relevant PLDs, but the temporal resolution of the ASL signal evolution will be higher.

The temporal SNR of te-pCASL PRESS approach applied to WM was found to be similar to the temporal SNR of the EPI readout. Although the study performed by Pohmann (8) claimed that a spectroscopy readout would result in increased sensitivity relative to traditional EPI, that study did not test this hypothesis experimentally, e.g. by a head-to-head comparison. The results of the current study show that the expected theoretical increase in SNR is difficult to achieve in practice. In addition, from a theoretical point of view, it can be considered to be difficult to predict which approach would be most sensitive as, on the one hand, a readout at the final analysis resolution should result in a higher SNR than *post-hoc* averaging over smaller voxels (16), whereas, on the other, imperfect shimming can result in signal cancelations showing as line broadening in ASL spectroscopy. Moreover, variations in labeling efficiency and physiological fluctuations in WM CBF could be the dominant noise sources for this application, whereas both of these sources of variation are independent of the readout resolution. In the context of our study, these effects seem to balance each other out, resulting in similar temporal SNRs. This will imply, for most experiments, a preference for the use of a conventional imaging readout for WM ASL experiments, because this will enable more irregular shaped ROIs for WM perfusion measurements, rather than the clinically available rectangular shaped ROI of the PRESS readout. By employing an irregular shaped ROI when analyzing perfusion images, partial volume effects can be minimized that could otherwise lead to the averaging of kinetic curves with different timing characteristics, resulting in quantification challenges. Moreover, measurements can be performed at multiple locations, such as the left and right hemisphere, increasing the relative efficiency of an imaging readout

even further. Although the current study implies that spectroscopic readout has a limited future in ASL for increasing sensitivity for WM perfusion measurement, one could speculate that ASL in combination with a spectroscopic readout would enable the monitoring of metabolic changes within or near the microvasculature. The limited SNR of such an approach will, however, be an important limitation.

In GM, the EPI approach showed higher ASL signal for the shortest PLDs compared with the PRESS spectroscopic readout. This can be explained by the detection of more vascular signal by the EPI readout, whereas such vascular signals would be suppressed for the ASL spectroscopy readout because of the temporal characteristics of the PRESS module: two spatially selective 180° pulses played out after the 90° excitation pulse, thus preventing flowing spins from being effectively excited. The higher contribution of the vascular signal to the te-pCASL EPI signal can also explain the observed shorter ATT of 1121 ± 118 ms obtained by te-pCASL EPI, compared with 1571 ± 297 ms as obtained by te-pCASL PRESS. Interestingly, the difference in WM ATTs between the two approaches (1571 ± 297 ms versus 1679 ± 408 ms) was much smaller and the statistical testing showed no significant difference for WM CBF or WM ATT obtained from the two approaches, which could be easily explained by the smaller vascular density in WM relative to that in GM. To better understand the observed differences between the PRESS and EPI readouts and to study the impact of vascular signal on the recorded ASL signals, te-pCASL EPI was performed with and without vascular crushing in a single volunteer (see Supporting Information). The results of this experiment confirm that vascular signal contamination can explain the observed differences in the patterns of the ASL signals between the spectroscopy and imaging readout: with vascular crushers, the maximum signal in GM is observed much later than without vascular crushers (at a PLD of 2000 ms versus approximately 1000 ms when no crushers are applied). When taking this effect into account, the GM measurements seem to indicate a higher SNR for the spectroscopy readout relative to the EPI readout, at between PLDs of 2000 and 4000 ms, te-pCASL PRESS shows higher perfusion signal and slightly higher temporal SNR than te-pCASL EPI. However, as this improved performance was not observed for the low-SNR application of WM perfusion measurements, our recommendation remains to rely on conventional imaging readouts for ASL.

Compared with te-pCASL PRESS, lower perfusion signal and faster decrease in GM were observed for te-pCASL EPI, especially for PLDs of 2000-4000 ms. This could potentially be explained by the fact that PRESS is less sensitive than gradient-echo EPI to T_2^* dephasing, and a spin-echo EPI would minimize this effect. This

difference in sensitivity could become more apparent when the labeled spins enter the microvasculature and cross from the intra- to the extravascular space. For these compartments, shorter T_2^* values are expected that would result in faster decay of the signal and thus decreased signal detection (17-19).

In this study of WM perfusion measurements, partial volume effects, i.e. GM contamination in the WM ROI, were avoided by careful planning of the PRESS voxel. Contamination of GM signal into WM perfusion signal would result in an artifactual increased WM CBF because of the much higher CBF in the GM. Outer volume suppression could further reduce GM contamination (8), but this was not implemented in the current study. So far, all te-pCASL PRESS scans have been performed with linear shimming, whereas higher order shimming might improve the temporal SNR by diminishing the field inhomogeneities over such a large voxel. It would, however, be essential that shimming of the labeling plane would not be affected by improved shimming of the readout region, as off-resonance effects could significantly reduce the labeling efficiency in pCASL (20).

One of the drawbacks of te-pCASL PRESS might be an increased sensitivity to motion. Because the PRESS readout does not provide any imaging data, retrospective motion correction could not be performed. To minimize motion artifacts, the volunteer's head was carefully immobilized using foam padding. Navigators (21) or optical tracking (22) might be additional solutions to limit the effects of motion, but these were considered to be beyond the scope of the current study. Another limitation of the current study is the use of EPI as the imaging readout, whereas three-dimensional readout approaches are considered to be the more optimal strategy. However, time-encoded pCASL relies on more than the conventional two conditions (i.e. perfusion-weighted and control condition) and is therefore more compatible with single-shot readout approaches. Single-shot three-dimensional sequences are more prone to blurring in the volume selection direction and therefore multi-slice two-dimensional EPI was chosen for the current study.

To conclude, time-encoded pCASL enables the measurement of multi-phase WM perfusion signals in a highly time-efficient manner compared with FAIR PRESS. te-pCASL PRESS can be used to measure localized WM perfusion changes, but it does not result in improved temporal SNR for WM perfusion measurements when compared with traditional te-pCASL EPI.

Supplementary Material

Methods

To investigate the impact of vascular contamination on the results of the ASL experiments in gray matter, one volunteer was scanned with and without vascular crushing using a T_1 adjusted te-pCASL scheme with a shorter total label-duration to account for the shorter transit time of gray matter (T_1-adjusting based upon the T_1 of blood (1650 ms) to achieve comparable SNR for all PLDs under the assumption that the label resides mostly intravascularly, Hadamard matrix of order 12, block durations of 894, 579, 429, 340 283, 241, 211, 187, 168, 153, 115 ms, PLD of 49 ms) (9). Background suppression pulses were played 1925 ms and 3120 ms after the start of labeling. The following parameters were used: single shot EPI, SENSE acceleration factor of 2.5, EPI factor of 31, spatial resolution of 3×3×7 mm^3, TE of 22 ms and water-fat shift of 10.12 pixels, the strength of the vascular crushers corresponded to a velocity-encoding of 5 cm/s in all directions.

Results

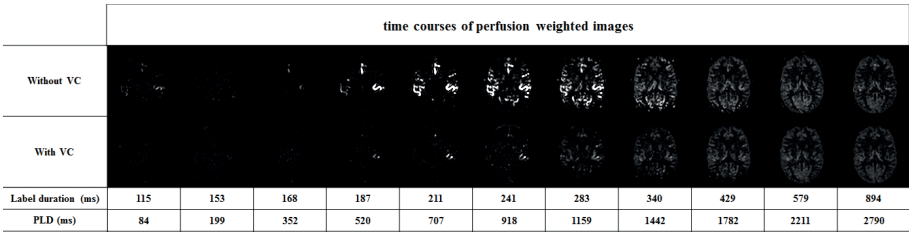

Label duration (ms)	115	153	168	187	211	241	283	340	429	579	894
PLD (ms)	84	199	352	520	707	918	1159	1442	1782	2211	2790

(a)

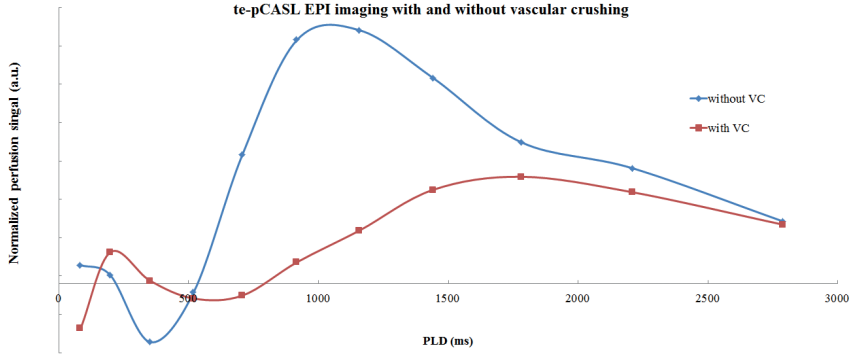

(b)

Figure S1: A) Perfusion weighted images for specific block durations and subsequent PLDs in a single volunteer acquired by te-pCASL EPI without (top) and with (bottom) vascular crushing. B) Time-course of the normalized perfusion signal in gray matter obtained by te-pCASL EPI without (blue) and with (red) vascular crushing.

Figure S1 shows time courses of the perfusion weighted images and normalized perfusion signal in gray matter obtained by te-pCASL EPI with and without vascular crushing. A higher perfusion signal at a very short post labeling delay was observed for the data acquired without vascular crushing.

References

1. Alsop DC, Detre JA, Golay X, Gunther M, Hendrikse J, Hernandez-Garcia L, Lu H, Macintosh BJ, Parkes LM, Smits M, van Osch MJ, Wang DJ, Wong EC, Zaharchuk G. Recommended implementation of arterial spin-labeled perfusion MRI for clinical applications: A consensus of the ISMRM perfusion study group and the European consortium for ASL in dementia. Magn Reson Med 2014.
2. Kluytmans M, van der Grond J, Folkers PJ, Mali WP, Viergever MA. Differentiation of gray matter and white matter perfusion in patients with unilateral internal carotid artery occlusion. J Magn Reson Imaging 1998;8(4):767-774.
3. De Keyser J, Steen C, Mostert JP, Koch MW. Hypoperfusion of the cerebral white matter in multiple sclerosis: possible mechanisms and pathophysiological significance. J Cereb Blood Flow Metab 2008;28(10):1645-1651.
4. Stanimirovic DB, Friedman A. Pathophysiology of the neurovascular unit: disease cause or consequence? J Cereb Blood Flow Metab 2012;32(7):1207-1221.
5. van Gelderen P, de Zwart JA, Duyn JH. Pittfalls of MRI measurement of white matter perfusion based on arterial spin labeling. Magn Reson Med 2008;59(4):788-795.
6. van Osch MJ, Teeuwisse WM, van Walderveen MA, Hendrikse J, Kies DA, van Buchem MA. Can arterial spin labeling detect white matter perfusion signal? Magn Reson Med 2009;62(1):165-173.
7. Mutsaerts HJ, Richard E, Heijtel DF, van Osch MJ, Majoie CB, Nederveen AJ. Gray matter contamination in arterial spin labeling white matter perfusion measurements in patients with dementia. Neuroimage Clin 2014;4:139-144.
8. Pohmann R. Accurate, localized quantification of white matter perfusion with single-voxel ASL. Magn Reson Med 2010;64(4):1109-1113.
9. Teeuwisse WM, Schmid S, Ghariq E, Veer IM, van Osch MJ. Time-encoded pseudocontinuous arterial spin labeling: basic properties and timing strategies for human applications. Magn Reson Med 2014;72(6):1712-1722.
10. Günther M. Highly efficient accelerated acquisition of perfusion inflow series by cycled arterial spin labeling. Proceedings of the 15th Annual Meeting of ISMRM, Berlin, Germany 2007;Abstract 380.
11. Ordidge RJ, Wylezinska M, Hugg JW, Butterworth E, Franconi F. Frequency offset corrected inversion (FOCI) pulses for use in localized spectroscopy. Magnetic Resonance in Medicine 1996;36(4):562-566.
12. Nehrke K, Bornert P, Groen J, Smink J, Bock JC. On the performance and accuracy of 2D navigator pulses. Magn Reson Imaging 1999;17(8):1173-1181.
13. Buxton RB, Frank LR, Wong EC, Siewert B, Warach S, Edelman RR. A general kinetic model for quantitative perfusion imaging with arterial spin labeling. Magnetic Resonance in Medicine 1998;40(3):383-396.
14. Herscovitch P, Raichle ME. What Is the Correct Value for the Brain Blood Partition-Coefficient for Water. Journal of Cerebral Blood Flow and Metabolism 1985;5(1):65-69.
15. Calamante F, Thomas DL, Pell GS, Wiersma J, Turner R. Measuring cerebral blood flow using magnetic resonance imaging techniques. Journal of Cerebral Blood Flow and Metabolism 1999;19(7):701-735.
16. Wong EC. Direct imaging of functional networks. Brain Connect 2014;4(7):481-486.
17. Wansapura JP, Holland SK, Dunn RS, Ball WS. NMR relaxation times in the human brain at 3.0 tesla. Journal of Magnetic Resonance Imaging 1999;9(4):531-538.
18. Liu P, Uh J, Lu H. Determination of spin compartment in arterial spin labeling MRI. Magn Reson Med 2011;65(1):120-127.
19. Schmid S, Teeuwisse WM, Lu H, van Osch MJ. Time-efficient determination of spin compartments by time-encoded pCASL T_2-relaxation-under-spin-tagging and its application in hemodynamic characterization of the cerebral border zones. Neuroimage 2015;123:72-79.
20. Dai WY, Garcia D, de Bazelaire C, Alsop DC. Continuous Flow-Driven Inversion for Arterial Spin Labeling Using Pulsed Radio Frequency and Gradient Fields. Magnetic Resonance in Medicine 2008;60(6):1488-1497.
21. Versluis MJ, Sutton BP, de Bruin PW, Bornert P, Webb AG, van Osch MJ. Retrospective image correction in the presence of nonlinear temporal magnetic field changes using multichannel navigator echoes. Magn Reson Med 2012;68(6):1836-1845.
22. Zaitsev M, Dold C, Sakas G, Hennig J, Speck O. Magnetic resonance imaging of freely moving objects: Prospective real-time motion correction using an external optical motion tracking system. Neuroimage 2006;31(3):1038-1050.